Bioresource Technology 120 (2012) 218–224

Contents lists available at SciVerse ScienceDirect

Bioresource Technology

journal homepage: www.elsevier.com/locate/biortech

Utilization of bivalve shell-treated *Zea mays* L. (maize) husk leaf as a low-cost biosorbent for enhanced adsorption of malachite green

A.A. Jalil [a,*], S. Triwahyono [b], M.R. Yaakob [a], Z.Z.A. Azmi [a], N. Sapawe [a], N.H.N. Kamarudin [a], H.D. Setiabudi [a], N.F. Jaafar [b], S.M. Sidik [b], S.H. Adam [a], B.H. Hameed [c]

[a] Institute of Hydrogen Economy, Faculty of Chemical Engineering, Universiti Teknologi Malaysia, 81310 UTM Skudai, Johor, Malaysia
[b] Ibnu Sina Institute for Fundamental Science Studies, Faculty of Science, Universiti Teknologi Malaysia, 81310 UTM Skudai, Johor, Malaysia
[c] School of Chemical Engineering, Engineering Campus, Universiti Sains Malaysia, 14300 Nibong Tebal, Penang, Malaysia

HIGHLIGHTS

- A low cost bivalve shell treated *zea mays* L. husk leaf biosorbent was developed.
- BS acts as a strong alkali pretreatment agent for ZHL.
- BS-ZHL enhanced the malachite green adsorption up to 81.5 mg g^{-1} (q_{max}).
- The experimental data agrees with the Langmuir isotherm model.
- The adsorption was controlled by the physisorption process.

GRAPHICAL ABSTRACT

ARTICLE INFO

Article history:
Received 18 April 2012
Received in revised form 18 June 2012
Accepted 23 June 2012
Available online 30 June 2012

Keywords:
Low-cost adsorbent
Bivalve shell
Zea mays L.
Malachite green
Isotherm

ABSTRACT

In this work, two low-cost wastes, bivalve shell (BS) and *Zea mays* L. husk leaf (ZHL), were investigated to adsorb malachite green (MG) from aqueous solutions. The ZHL was treated with calcined BS to give the BS-ZHL, and its ability to adsorb MG was compared with untreated ZHL, calcined BS and $Ca(OH)_2$-treated ZHL under several different conditions: pH (2–8), adsorbent dosage (0.25–2.5 g L^{-1}), contact time (10–30 min), initial MG concentration (10–200 mg L^{-1}) and temperature (303–323 K). The equilibrium studies indicated that the experimental data were in agreement with the Langmuir isotherm model. The use of 2.5 g L^{-1} BS-ZHL resulted in the nearly complete removal of 200 mg L^{-1} of MG with a maximum adsorption capacity of 81.5 mg g^{-1} after 30 min of contact time at pH 6 and 323 K. The results indicated that the BS-ZHL can be used to effectively remove MG from aqueous media.

1. Introduction

There is a growing recognition that malachite green (MG) should be removed from effluents to protect water resources because MG potentially has harmful effects on the liver, gills, kidneys, intestines and gonads of organisms (Daneshvar et al., 2007). Among the existing physical, chemical and biological methods, adsorption is the most commonly used method to remove dyes from water because adsorption is low cost, has a simple design, is easy to perform, is insensitive to toxic substances and can completely remove dyes, even from dilute solutions (Bingöl et al., 2012). Adsorption onto activated carbon, the most popular technique, has been used with great success. However, adsorbent-grade activated carbon is expensive, and the regeneration of activated carbon for reuse increases the cost (Gong et al., 2009). Therefore, there is growing interest in identifying more low-cost and effective alternatives to activated carbon, such as agro-industry waste (Abidin et al., 2011; Rahman et al., 2005), algae (Dotto et al., 2012), zeolite (Han et al., 2010) and sludge (Ong et al., 2010). However, the adsorption capacities of most of the

* Corresponding author. Tel.: +60 7 5535581; fax: +60 7 5581463.
E-mail address: aishah@cheme.utm.my (A.A. Jalil).

0960-8524/$ - see front matter © 2012 Elsevier Ltd. All rights reserved.
http://dx.doi.org/10.1016/j.biortech.2012.06.066

reported adsorbents remain limited. The development of a cheap and extensively available resource as an alternative adsorbent is essential for the efficient removal of dyes from industrial wastewater. In addition, the use of waste material as an adsorbent would minimize the total amount of waste, which is a step towards a more "earth-friendly" process.

Zea mays L. (i.e., maize) husk leaf (ZHL) is a lignocellulosic-rich agricultural waste that is abundantly available throughout the year. However, ZHL is allowed to decompose in fields or burned without being used effectively, which may cause pollution that affects the ecosystem unfavorably. Bivalve shell (BS), another abundant and non-edible waste, is mainly composed of calcium carbonate and is found in many coastal areas; therefore, economically recycling and reusing this pollution-causing waste is desirable. In general, finding uses (especially on a large scale) for these abundant waste materials would be profitable from both an environmental and economic point of view. Herein, we report the use of crushed BS as an agent to treat ZHL to enhance the removal of MG from aqueous solution through adsorption. The conversion of two wastes, as opposed to the use of commercially available compounds, into materials that can potentially improve the environment would be advantageous in response to ecological constraints for the sustainable development of industries using dyes. Additionally, this research can potentially extend the application of the abundant ZHL and BS materials beyond animal feed and ornamentation, respectively. The adsorption of MG was studied under several different experimental conditions, including pH, adsorbent dosage, contact time, initial MG concentration and temperature. The equilibrium, kinetics and thermodynamics of the adsorption process were also investigated.

2. Methods

2.1. Materials

The ZHL and BS were collected from the nearest corn farm and beach at Johor, respectively. The highest available grades of $Ca(OH)_2$ and malachite green (MG) oxalate [C.I. Basic Green 4, C.I. Classification Number 42,000, purity >90%, chemical formula = $C_{52}H_{54}N_4O_{12}$, MW = 927.00, λ_{max} = 618 nm] were purchased from Sigma Aldrich (M) (Sdn Bhd, Malaysia) and were used as received (i.e., without purification).

2.2. Preparation of adsorbent

The green-colored ZHLs were chopped into pieces that were 1–2 cm in length, and then the pieces were soaked in water overnight to remove any impurities adhering to the surface before the pieces were oven-dried at 80 °C for 24 h. The pieces were blended and sieved to a consistent size of 355–600 μm, and then the pieces were oven-dried at 100 °C overnight until the weights were constant. Finally, the pieces were stored in a plastic bottle. The BS samples were washed with water, oven-dried at 80 °C, crushed and sieved to a powder with a size of 355–600 μm. The resultant BS powder was subsequently calcined overnight at 550 °C.

Pretreatment of the ZHL with $Ca(OH)_2$ was accomplished by adding 8.6 g of $Ca(OH)_2$ into 1 L of water that contained 10 g of powdered ZHL. The mixture was stirred for 4 h at room temperature, filtered and oven-dried at 80 °C overnight. A similar procedure was followed for the treatment of ZHL with raw and calcined BS that was crushed.

The zero point charge (pH_{zpc}) of the BS-ZHL was determined using the powder addition method, which was previously reported in the literature (Çelekli et al., 2009).

2.3. Characterization of ZHL and BS

The infrared spectra of the ZHL sample were obtained using a Fourier-transform infrared spectrometer (Spectrum GX, Perkin Elmer, USA). The samples were prepared as KBr pellets and scanned over the range of 4000–400 cm^{-1} to identify the functional groups that were responsible for adsorption. The morphological features and surface characteristics of the samples were obtained from a field emission scanning electron microscopy (FESEM) using a JEOUL JSM-6701F scanning electron microscope at an accelerating voltage of 15 kV. The samples were coated with platinum by electro-deposition under vacuum prior to analyses. The composition of crushed seashell was determined on a Bruker AXS (S4 Pioneer) X-ray fluorescence spectrometer. The absorbance measurements of the dyes decolorization was monitored by UV/vis spectrophotometer (Thermo Scientific Genesys 10UV Scanning).

2.4. Adsorption experiments

The dye solution of MG was prepared by dissolving accurately measured amounts of MG in Milli-Q water to obtain a concentration of 1000 mg L^{-1}, and then the solution was diluted to various concentrations. Adsorption experiments were performed by adding 0.1 g of calcined BS treated ZHL (BS-ZHL) in a 250 mL conical flask containing 200 mL of a 10 mg L^{-1} MG solution. The pH of the working solutions was adjusted to the desired value with HCl or NaOH. The mixtures were prepared under constant stirring at a rate of 300 rpm at room temperature (30 °C) to reach equilibrium. The samples were then withdrawn at appropriate time intervals and centrifuged at 3500 rpm for 15 min. The residual MG concentration was determined using a UV/vis spectrophotometer at 618 nm. All experiments were performed in triplicate.

At any time, t, the adsorption capacity of MG adsorbed (q_t, mg g^{-1}) on BS-ZHL was calculated by the following mass-balance equation,

$$q_t = \frac{(C_o - C_t)}{W} \times V \quad (1)$$

The MG removal percentage can be calculated as follows,

$$\text{Removal } (\%) = \left(\frac{C_o - C_t}{C_t}\right) \times 100 \quad (2)$$

3. Results and discussion

3.1. Characterization of adsorbent

The X-ray fluorescence (XRF) results for the calcined BS are shown in Supplementary Table 1. CaO was determined to be the major constituent of the calcined BS (98%), while trace amounts of other oxides were also present. The results indicate that BS is a good natural, low-cost, basic substitute for commercial $Ca(OH)_2$ for this study. Additionally, crushed BS, which is essentially calcium carbonate, decomposed to calcium oxide through calcination (Eq. (3)) and then converted to calcium hydroxide upon contact with water (Eq. (4)).

$$CaCO_3 \rightarrow CaO + CO_2 \quad (3)$$

$$CaO + H_2O \rightarrow Ca^{2+} + 2OH^- \quad (4)$$

The determination of the chemical structure of ZHL before BS pretreatment, after BS pretreatment, before MG adsorption and after MG adsorption could possibly identify the functional groups involved in the binding mechanism between the treated adsorbent and MG. FTIR spectra of untreated ZHL, $Ca(OH)_2$-treated ZHL,

BS-ZHL and BS-ZHL after adsorption of MG are shown in Supplementary Fig. 1. The wide band observed at 3450 cm^{-1} indicates that free and intermolecular bonded O–H groups were present, whereas the band at 2950 cm^{-1} was assigned as the stretching vibration of the C–H groups that were present in the lignin structure (Hameed and El-Khaiary, 2008a). The band observed at approximately 2364 cm^{-1} may correspond to an N–H stretching vibration, and the bands observed at approximately 1577 cm^{-1} and 1464 cm^{-1} indicated that C=C bonds of aromatic rings were present. The band at 1388 cm^{-1} was attributed to deformation of CH_3 groups, and the band at 802 cm^{-1} indicated that an aromatic amine was present (Parshetti et al., 2006). After adsorption of MG, the weak interactions between the BS-ZHL surface and MG was evidenced by a shift in the O–H and C=O bands from 3450 cm^{-1} and 1659 cm^{-1} to 3469 cm^{-1} and 1665 cm^{-1}, respectively (Sekhar et al., 2009). These results provide strong evidence for the adsorption of MG onto the BS-ZHL surface.

The surface structure of ZHL before and after BS pretreatment, as well as the BS-ZHL after MG adsorption, was analyzed using field-emission scanning electron microscopy (FE-SEM). As shown in Supplementary Fig. 2, the surface of ZHL was smooth before treatment with the BS; however, the surface was corroded and coarse after treatment, which indicates that the BS-ZHL surface has a higher tendency to trap and adsorb the dye. The structure of the BS-ZHL changed significantly after MG was adsorbed; the surface appeared to swell.

3.2. Effect of adsorbent pretreatment

Fig. 1 shows the effects of the various adsorbents on the removal of MG. Untreated ZHL was compared with raw BS, $Ca(OH)_2$-treated ZHL and BS-ZHL. The adsorption of untreated ZHL and raw BS resulted in 57% and 45% removal of MG, respectively. However, the percent of MG that was removed increased to 98% using Ca-ZHL and BS-ZHL after 30 min of contact time. One possible explanation for the increase in the percentage of MG removed is the increase in the electronegativity of both materials (i.e., Ca-ZHL and BS-ZHL) upon treatment with basic materials (i.e., $Ca(OH)_2$ and BS). Notably, the results indicate that BS can potentially be used as a low-cost pretreatment alternative to the commercial compound, calcium hydroxide.

3.3. Effect of pH

Investigation of the effects of initial pH on the adsorption of the dye is important because industrial dye wastewater is discharged at a pH that differs from the environmental pH. In this study, the effects of the initial pH of MG solutions were examined over a pH range of 2–8, and the results are presented in Fig. 2a. The adsorption uptakes at equilibrium were lower under conditions that were highly acidic and became higher as the pH increased; the maximum adsorption efficiency was achieved at pH 6 (20 mg g^{-1}). This behavior can be described on the basis of zero point charge (pH_{zpc}) of the BS-ZHL, which was determined to be at pH 5.5 (Supplementary Fig. 3). The H^+ ions effectively competed with the MG cations, which caused dye uptake to be lower at pHs less than the pH_{zpc}. However, at pHs higher than the pH_{zpc}, the surface of the BS-ZHL became negatively charged and electrostatically adsorbed the positively charged MG cations (Çelekli et al., 2009). This effect can be observed from the rapid increase in MG uptake from 8 to 20 mg g^{-1} at pH 2 to 6, respectively. The adsorption was also favorable at pH 8; however, the MG became unstable and might have formed a leuco compound (Chen et al., 2007). Therefore, pH 6 was determined to be the optimum pH value in this study.

3.4. Effect of adsorbent dosage

Fig. 2b shows the effect of the BS-ZHL dosage (0.25–2.5 g L^{-1}) on the adsorption of MG. The adsorption capacity increased as the adsorbent dosage decreased. A maximum adsorption uptake at equilibrium of 36.4 mg g^{-1} was obtained for a BS-ZHL dosage of 0.25 g L^{-1}. As the adsorbent dosage decreased, the number of unsaturated adsorption sites decreased, which resulted in a higher number of MG ions adsorbed per unit surface area of adsorbent.

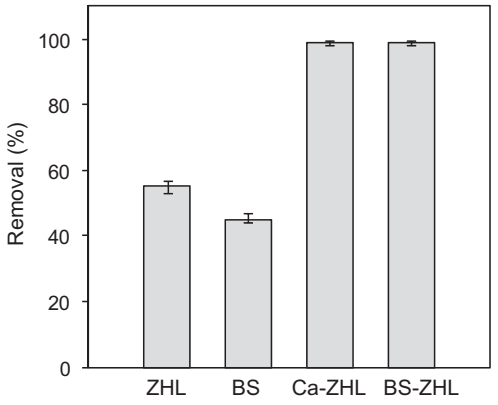

Fig. 1. Effect of pretreatment of ZHL on the removal of MG (Adsorbent: 2.5 g L^{-1}, MG initial concentration: 50 mg L^{-1}, pH 6, 303 K, 30 min).

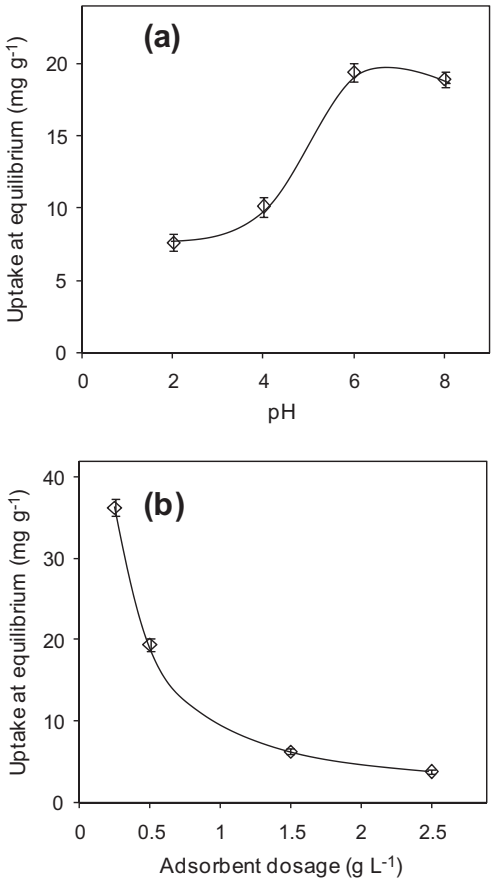

Fig. 2. Effect of initial pH (a) and BS-ZHL dosage (b) on the adsorption of MG onto BS-ZHL (Adsorbent: 0.5 g L^{-1}, pH 6, MG initial concentration: 10 mg L^{-1}, 303 K, 60 min).

3.5. Kinetic studies and adsorption mechanisms

Investigation of the adsorption kinetics is important in the treatment of aqueous effluents because the adsorption kinetics provide valuable information regarding the mechanism of the adsorption process. Two well-known, commonly used models to describe the adsorption behavior of pollutants on solid surfaces are the Lagergren pseudo-first-order (Lagergren, 1898) and the Ho pseudo-second-order (Ho and McKay, 1999) models. After application of the models, the Weber-Morris intraparticle diffusion model (Weber and Morris, 1963) was applied to analyze the kinetic results to determine the adsorption mechanism of the MG onto the BS-ZHL. The non-linear forms of the pseudo-first- and -second-order models and the linear form of intraparticle diffusion models are expressed as follows:

$$\text{Pseudo-first-order equation}: \quad q = q_e(1 - e^{-k_1 t}) \tag{5}$$

$$\text{Pseudo-second-order equation}: \quad q = \frac{q_e^2 k_2 t}{1 + q_e k_2 t} \tag{6}$$

$$\text{Weber-Morris equation}: \quad q_t = k_{id} t^{1/2} + C \tag{7}$$

For the non-linear regression method, the experimental data of the dye uptakes (q) versus time (t) were fitted to the models using the *solver* add-in with Microsoft's spreadsheet, Excel (Microsoft) (Ho et al., 2005). Table 1 lists both the rate constants (k_1 and k_2) and the corresponding non-linear regression correlation coefficient values (R^2) for both models for seven different initial concentrations of MG. Under all conditions studied, the values of R^2 for the pseudo-first-order models were greater than the pseudo-second-order models ($R^2 \geqslant 0.998$, Fig. 3a). These results indicate that the adsorption of MG onto the BS-ZHL could be better explained using the pseudo-first-order kinetics model (Hameed and El-Khaiary, 2008a).

From the kinetic studies, the adsorption of MG onto BS-ZHL has been predicted to be diffusion-controlled. Generally, there are several adsorption steps involved in the transfer of a solute in adsorption dynamics: the movement of the adsorbate molecules from the bulk solution to the external surface of the adsorbent (film diffusion), the movement of the adsorbate molecules to the interior regions of the adsorbent (particle diffusion) and the sorption of the solute on the interior surfaces of the pores of the adsorbent (sorption). The film diffusion is referred to as the boundary layer diffusion, which is characterized by external mass transfer. The particle diffusion is known as intraparticle diffusion. One or any combination of the three steps may be rate limiting (Benyousef and Amrani, 2011).

Analysis of the experimental kinetics results using the Weber and Morris intraparticle diffusion model is illustrated in Fig. 3b. The plots for the adsorption of 10, 30, 50, 70, 100, 150 and 200 mg L^{-1} of MG using BS-ZHL did not pass through the origin ($C = 0$) and were not linear over the entire time range, which implies that intraparticle diffusion was not the sole rate-limiting step.

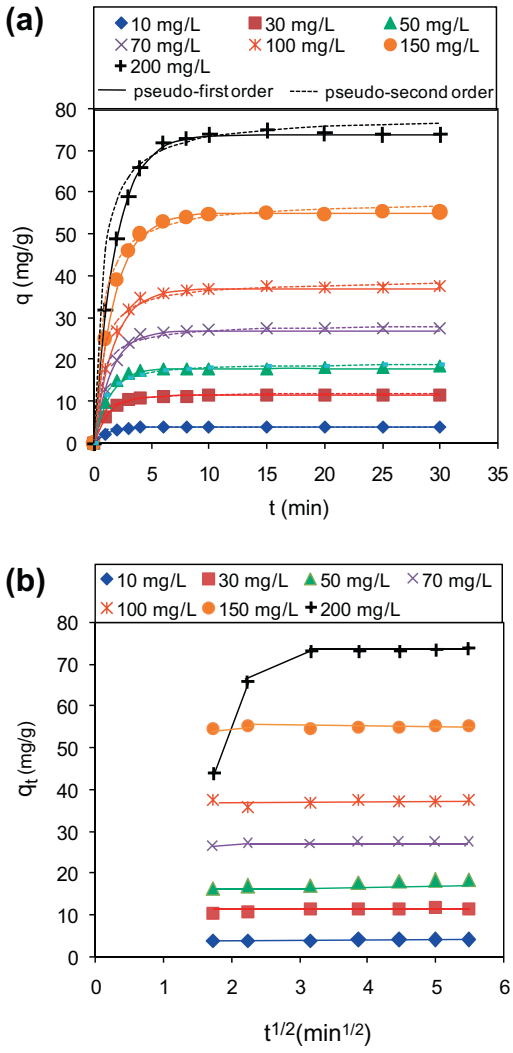

Fig. 3. Adsorption kinetics and their modeling at different initial concentrations. (Adsorbent: 2.5 g L^{-1}, pH 6, 323 K, 30 min).

A rapid increase in the uptake rate to the maximum adsorption capacities at equilibrium was observed at lower concentrations of MG, which demonstrated that the uptake of MG ions by the BS-ZHL surface was very fast: the rates of the pseudo-first-order model (k_1) shown in Table 1 increased as the initial MG concentrations decreased. At higher initial concentrations of MG (e.g., 150 mg L^{-1} and 200 mg L^{-1}), the adsorption appeared to be a multistep process, which was most likely due to molecular collisions in the highly concentrated MG solutions. Therefore, the movement of MG ions towards the heterogeneous BS-ZHL surface was hindered. In addition, the C values increased from 3.89 to 46.1 (data not

Table 1
Coefficient of pseudo-first and -second order adsorption kinetic models.

Initial conc. (mg L^{-1})	$q_{e,exp}$ (mg g^{-1})	Pseudo-first order			Pseudo-second order		
		q_e (mg g^{-1})	k_1 (min^{-1})	R^2	q_e (mg g^{-1})	k_2 (g/mg min)	R^2
10	4.07	4.01	0.832	0.999	4.11	0.802	0.995
30	11.7	11.5	0.766	0.999	12.3	0.144	0.998
50	18.5	18.0	0.716	0.999	19.2	0.081	0.990
70	27.4	26.9	0.665	0.999	28.5	0.059	0.992
100	37.5	37.0	0.581	0.999	39.0	0.038	0.993
150	55.2	55.1	0.551	0.999	57.8	0.026	0.994
200	73.9	73.9	0.542	0.998	78.4	0.018	0.993

shown) as the initial concentration of MG increased from 10 to 200 mg L^{-1}, which indicates that the boundary layer thicknesses and effects increased as the initial MG concentration increased. Therefore, in this study, the adsorption processes may have involved the diffusion of the MG ions from the bulk solution to the boundary layer, the diffusion of the MG ions from the external layer to the surface of BS-ZHL, the internal diffusion of the MG ions within the micro- and macro-pores and, finally, the sorption of MG ions on the interior BS-ZHL surfaces at the available sites (Metcalf and Eddy, 2003). The rate of the final stage began to decrease because equilibrium was achieved after most of the adsorption sites were saturated (Jalil et al., 2010).

3.6. Adsorption equilibrium studies

The effects of the initial concentration of MG adsorbed onto BS-ZHL were studied at different initial MG concentrations, ranging from 10 to 200 mg L^{-1} (Fig. 3a). The adsorption uptake at equilibrium increased with increasing initial dye concentrations and a maximum adsorption capacity of 74 mg g^{-1} was attained at a MG concentration of 200 mg L^{-1} after 30 min of contact time. High initial dye concentrations led to an increase in the mass gradient between the solution and the BS-ZHL, which functioned as the driving force for the transfer of dye ions from the bulk solution to the adsorbent surface (Jalil et al., 2010).

In this study, three commonly used isotherms were employed: the Langmuir (Langmuir, 1918), the Freundlich (Freundlich, 1906) and the Temkin (Temkin and Pyzhev, 1940). The non-linear regressions of the isotherm models can be represented by the following expressions (Foo and Hameed, 2012):

$$\text{Langmuir isotherm}: \quad q_e = \frac{q_m K_L C_e}{1 + K_L C_e} \tag{8}$$

$$\text{Freundlich isotherm}: \quad q_e = K_F C_e^{1/n_F} \tag{9}$$

$$\text{Temkin isotherm}: \quad q_e = B \ln(A C_e) \tag{10}$$

where C_e is the MG concentration at equilibrium (mg L^{-1}), q_e is the adsorption capacity at equilibrium (mg g^{-1}), q_m is the maximum adsorption capacity (mg g^{-1}), K_L is the Langmuir constant (L mg^{-1}), K_F is the Freundlich adsorbent capacity, n_F is the heterogeneity factor, A is the Temkin equilibrium binding constant (L g^{-1}) and B is the Temkin constant.

The validity of the models was verified by the root-mean-square deviation (RMSD), the commonly used statistical tool measuring the predictive power of a model, which is expressed as

$$\text{RMSD} = \frac{\sqrt{\sum_{i=1}^{n} (q_{exp} - q_p)^2}}{n - 1} \tag{11}$$

where q_{exp} and q_p are the experimental and theoretical adsorption capacities (mg g^{-1}), respectively (Hameed and El-Khaiary, 2008b).

Fig. 4 shows the plotted models, and the isotherm information extracted from the models is summarized in Table 2. The Langmuir isotherm model had the best fit with the experimental data due to the highest regression coefficient (R^2 = 0.998) and lowest RMSD value (RMSD = 0.308) compared to other isotherm models. This result indicates that the adsorption of MG onto the surface of BS-ZHL occurs as a monolayer; therefore, each molecule had equal enthalpies and activation energies (Hameed and El-Khaiary, 2008b).

The favorability of the adsorption could also be demonstrated by the value of essential characteristics of the Langmuir isotherm (R_L), which is a dimensionless constant that is the separation factor. The R_L can yield an isotherm shape that is unfavorable

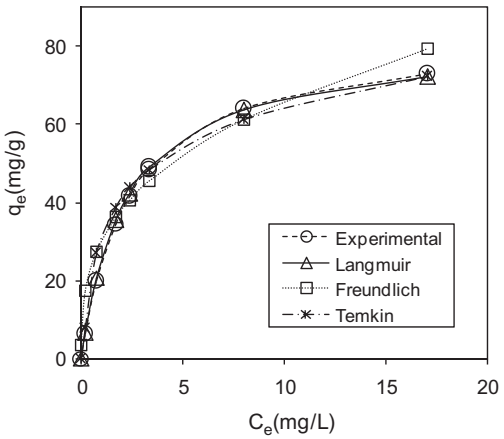

Fig. 4. Adsorption isotherms for the adsorption of MG onto BS-ZHL (Adsorbent: 2.5 g L^{-1}, pH 6, 303 K, 30 min).

Table 2
Isotherm parameters for adsorption of MG onto BS-ZHL at 323 K.

Isotherm	Parameters
Langmuir	
q_m (mg g^{-1})	81.5
K_L (L mg^{-1})	0.449
R^2	0.998
RMSD	0.308
Freundlich	
n	2.93
K_F (mg g^{-1}) (L mg^{-1})$^{1/n}$	30.1
R^2	0.944
RMSD	0.381
Temkin	
B	14.5
A (L g^{-1})	8.49
R^2	0.999
RMSD	0.895

($R_L > 1$), linear ($R_L = 1$), favorable ($0 < R_L < 1$) or irreversible ($R_L = 0$). Using the following equation (Inbaraj et al., 2009),

$$R_L = \frac{1}{1 + K_L C_0} \tag{12}$$

the R_L value for the system was calculated to be 0.011, which indicates that favorable adsorption of MG occurred with the maximum adsorption capacity being 81.5 mg g^{-1}. As compared with data reported in the literature (Table 3), the BS-ZHL had a relatively higher adsorption capacity than various other natural biomasses. Modified rice straw was reported to have a higher adsorption capacity; however, the adsorption time was 20 times longer than the contact time used for the BS-ZHL in this study [Gong et al., 2006].

The Temkin adsorption potential (A) of BS-ZHL for MG was 8.49, which indicates the biomass-dye ion potential was relatively high. The reason for the high value was most likely the electrostatic attraction between the materials (Horsfall and Spiff, 2005). The Temkin constant (b), which is related to the heat of sorption ($B = RT/b$) of MG was 0.347 kJ mol^{-1}. This result indicates that the interaction between the sorbate and sorbent (physisorption) was weak because the typical range of bonding energy for an ion-exchange mechanism (chemisorption) is 8–16 kJ mol^{-1} (Ho et al., 2002).

Table 3
Comparison of MG adsorption capacities of BS-ZHL with other reported adsorbents.

Adsorbent	Contact time (h)	pH	Adsorbent dosage (g L^{-1})	q_m (mg g^{-1})	References
Bivalve shell-*z. mays* L. husk leaf (BS-ZHL)	0.5	6	2.5	81.5	This study
Chitosan bead	5	8	10	94	Hameed and El-Khaiary (2008b)
Cellulose	0.5	7	5	2.42	Sekhar et al. (2009)
Activated carbon from rice husk	0.5	5	6	57.1	Rahman et al. (2005)
Lemon Peel	24	–	0.5	51.7	Metcalf and Eddy (2003)
Degreased coffee bean	1	4	2	55.3	Ong et al. (2010)
Sea shell powder	2	8	2	42.3	Pan et al. (2012)
Fresh water algae	1	5	1	64	Patel and Suresh (2008)
Marine alga	6	–	4	21.7	Chen et al. (2007)
Arundo donax root carbon	3	5	6	8.69	Hameed and El-Khaiary (2008a)
Modified rice straw	10	4	2	256	Gong et al. (2006)
Anaerobic granular sludge	2	5	2.4	59.2	Cheng et al. (2008)

(Initial MG Concentration: 10–300 mg L^{-1}, 303–323 K).

Table 4
Thermodynamic parameters for the adsorption of MG onto BS-ZHL.

Temp (K)	K_c	ΔG^o (kJ mol^{-1})	ΔH^o (kJ mol^{-1})	ΔS^o (J mol^{-1} K^{-1})	E_a (kJ mol^{-1})
303	11.2	−5.93	32.4	127	21.5
313	14.0	−7.19			
323	24.9	−8.46			

(200 mg L^{-1}, pH 6, 2.5 g L^{-1}, 30 min).

3.7. Thermodynamic studies

The thermodynamic parameters were evaluated to investigate the nature of the adsorption. Investigation of the effects temperature (303–323 K) had on the adsorption of MG onto BS-ZHL indicated that the adsorption capacity of the MG increased as the temperature increased; therefore, the process was endothermic. The adsorption enthalpy (ΔH^o), entropy (ΔS^o) and Gibbs free energy (ΔG^o) were calculated using the following thermodynamic functions:

$$\ln K_c = \frac{\Delta S^o}{R} - \frac{\Delta H^o}{RT} \tag{13}$$

$$K_c = \frac{C_e(\text{adsorbent})}{C_e(\text{solution})} \tag{14}$$

$$\Delta G^0 = -RT \ln K_c \tag{15}$$

where K_c is the equilibrium constant of the adsorption. The plot of $\ln K_c$ versus $1/T$ (figure not shown) resulted in a straight line with a slope of ΔH^o (kJ mol^{-1}) and an intercept of ΔS^o (kJ mol^{-1} K^{-1}). The values of these thermodynamic parameters were determined at three different temperatures, which are listed in Table 4. The overall ΔG^o during the adsorption was negative for the range of temperatures investigated, which decreased in magnitude as the temperature increased. This may correspond to a reduction in the degree of spontaneity at elevated temperatures. The positive value of ΔH^o indicates that the adsorption process was endothermic and that the magnitude (32.4 kJ mol^{-1}) was in the heat range of physisorption (<40 kJ mol^{-1}) (Wang et al., 2010). This result was in agreement with the kinetic experiments performed at various temperatures discussed previously. Therefore, as the temperature increased, more active sites upon the BS-ZHL were available, which resulted in an enhancement in adsorption due to the increase in surface activity and kinetic energy of the MG molecules. The positive value of ΔS^o (127 J K^{-1} mol^{-1}) corresponds to an increase in the randomness at the solid-solute interface, which indicates that the affinity of MG toward the adsorbent was high. This result most likely reflects structural changes in the sorbate and adsorbent. Similar results were reported in the literature (Pan et al., 2012; Aksu and Karabayir, 2008; Patel and Suresh, 2008).

The activation energy (E_a) is defined as the minimum kinetic energy required by the sorbate ions to react with the active sites available on the surface of the adsorbent. The value of E_a can be obtained by the Arrhenius equation,

$$\ln k_2 = \ln A - \frac{E_a}{R}\left(\frac{1}{T}\right) \tag{16}$$

The slope of the plot of $\ln k_2$ versus $1/T$ resulted in a value for the E_a that was 21.5 kJ mol^{-1} (Table 4). Generally, low activation energies (5–40 kJ mol^{-1}) are characteristic of physical adsorption, whereas high values (40–800 kJ mol^{-1}) are characteristic of chemisorptions (Dogan et al., 2006). Therefore, the MG adsorption onto BS-ZHL was a physical adsorption process.

4. Conclusion

The present study demonstrated that BS-ZHL can be used as an effective adsorbent for the removal of MG from aqueous solutions. Besides minimizing wastes, the results also provide additional benefits to industrial dye wastewater treatment. Pretreatment of the raw ZHL with BS effectively enhanced its electronegativity, which led to an increased adsorption capacity. The results indicated that the experimental data were fitted well to Langmuir isotherm model. The kinetics of adsorption followed a pseudo-first-order model. The thermodynamic studies provided evidence for the feasibility, spontaneity and endothermic nature of the adsorption process, which is controlled by a physisorption process.

Acknowledgements

We gratefully acknowledged the financial support by a Fundamental Research Grant from the Ministry of Higher Education Malaysia (Vot No. 78326). We are also thankful to The Hitachi Scholarship Foundation for their supports and advice.

Appendix A. Supplementary data

Supplementary data associated with this article can be found, in the online version, at http://dx.doi.org/10.1016/j.biortech.2012.06.066.

References

Abidin, M.A.Z., Jalil, A.A., Triwahyono, S., Adam, S.H., Kamarudin, N.H.N., 2011. Recovery of gold(III) from an aqueous solution onto a durio zibethinus husk. Biochem. Eng. J. 54, 124–131.

Aksu, Z., Karabayir, G., 2008. Comparison of biosorbent properties of different kinds of fungi for the removal of Gryfalan Black RL metal-compex dye. Bioresour. Technol. 99, 7730–7741.

Benyousef, S., Amrani, M., 2011. Removal of phosphorus from aqueous solutions using chemically modified sawdust of *Aleppo pine* (*Pinus halepensis Miller*): kinetics and isotherm studies. Environmentalist 31, 1–8.

Bingöl, D., Hercan, M., Elevli, S., Kılıç, E., 2012. Comparison of the results of response surface methodology and artificial neural network for the biosorption of lead using black cumin. Bioresour. Technol. 112, 111–115.

Çelekli, A., Yavuzatmaca, M., Bozkurt, H., 2009. Kinetic and equilibrium studies on the adsorption of reactive red 120 from aqueous solution on *Spirogyra majuscula*. Chem. Eng. J. 152, 139–145.

Chen, C.C., Lu, C.S., Chung, Y.C., Jan, J.L., 2007. UV light induced photodegradation of malachite green on TiO_2 nanoparticles. J. Hazard. Mater. 141, 520–528.

Cheng, W., Wang, S.-G., Lu, L., Gong, W.-X., Liu, X.-W., Gao, B.-Y., Zhang, H.-Y., 2008. Removal of malachite green (MG) from aqueous solutions by native and heat-treated anaerobic granular sludge. Biochem. Eng. J. 39, 538–546.

Daneshvar, N., Ayazloo, M., Khataee, A.R., Pourhassan, M., 2007. Biological decolorization of dye solution containing Malachite Green by microalgae *Cosmarium* sp. Bioresour. Technol. 98, 1176–1182.

Dogan, M., Alkan, M., Demirbas, O., Ozdemir, Y., Ozmetin, C., 2006. Adsorption kinetics of maxilon blue GRL onto sepiolite from aqueous solutions. Chem. Eng. J. 124, 89–101.

Dotto, G.L., Lima, E.C., Pinto, L.A.A., 2012. Biosorption of food dyes onto *Spirulina platensis* nanoparticles: equilibrium, isotherm and thermodynamic analysis. Bioresour. Technol. 103, 123–130.

Foo, K.Y., Hameed, B.H., 2012. Mesoporous activated carbon from wood sawdust by K_2CO_3 activation using microwave heating. Bioresour. Technol. 111, 425–432.

Freundlich, H.M.F., 1906. Uber die adsorption in lösungen. Z. Phys. Chem. 57, 385–470.

Gong, R., Feng, M., Zhao, J., Cai, W., Liu, L., 2009. Functionalization of sawdust with monosodium glutamate for enhancing its malachite green removal capacity. Bioresour. Technol. 100, 975–978.

Gong, R., Jin, Y., Chen, F., Chen, J., Liu, Z., 2006. Enhanced malachite green removal from aqueous solution by citric acid modified rice straw. J. Hazard. Mat. 137, 865–870.

Hameed, B.H., El-Khaiary, M.I., 2008a. Batch removal of malachite green from aqueous solutions by adsorption on oil palm trunk fibre: equilibrium isotherms and kinetic studies. J. Hazard. Mater. 154, 237–244.

Hameed, B.H., El-Khaiary, M.I., 2008b. Equilibrium, kinetics and mechanism of malachite green adsorption on activated carbon prepared from bamboo by K_2CO_3 activation and subsequent gasification with CO_2. J. Hazard. Mater. 157, 344–351.

Han, R., Wang, Y., Sun, Q., Wang, L., Song, J., He, X., Dou, C., 2010. Malachite green adsorption onto natural zeolite and reuse by microwave irradiation. J. Hazard. Mater. 175 (1–3), 1056–1061.

Ho, Y.S., McKay, G., 1999. Pseudo-second order model for sorption processes. Process Biochem. 34, 451–465.

Ho, Y.-S., Chiu, W.-T., Wang, C.-C., 2005. Regression analysis for the sorption isotherms of basic dyes on sugarcane dust. Bioresour. Technol. 96, 1285–1291.

Ho, Y.S., Porter, J.F., McKay, G., 2002. Equilibrium isotherm studies for the sorption of divalent metal ions onto peat: copper, nickel and lead single component systems. Water, Air, and Soil Pollut. 141, 1–33.

Horsfall Jr., M., Spiff, A.I., 2005. Equilibrium sorption study of Al^{3+}, Co^{2+} and Ag^{+} in aqueous solutions by fluted pumpkin (Telfairia occidentalis HOOK f) waste biomass. Acta Chim Slov. 52, 174–181.

Inbaraj, B.S., Wang, J.S., Lu, J.F., Siao, F.Y., Chen, B.H., 2009. Adsorption of toxic mercury(II) by an extracellular biopolymer poly(c-glutamic acid). Bioresour. Technol. 100, 200–207.

Jalil, A.A., Triwahyono, S., Adam, S.H., Rahim, N.D., Aziz, M.A.A., Hairom, N.H.H., Razali, N.A.M., Abidin, M.A.Z., Mohamadiah, M.K.A., 2010. Adsorption of methyl orange from aqueous solution onto calcined Lapindo volcanic mud. J. Hazard. Mater. 181, 755–762.

Lagergren, S., 1898. About the theory of so-called adsorption of soluble substances. Kungliga Svenska Vetenskapsakademiens, Handlingar 24, 1–39.

Langmuir, I., 1918. The adsorption of gases on plane surfaces of glass, mica and platinum. J. Am. Chem. Soc. 40, 1361–1403.

Metcalf, Eddy, 2003. Wastewater Engineering: Treatment and Reuse. McGraw Hill International Edition, New York, 478–483.

Ong, S.-A., Uchiyama, K., Inadama, D., Ishida, Y., Yamagiwa, K., 2010. Treatment of azo dye Acid Orange 7 containing wastewater using up-flow constructed wetland with and without supplementary aeration. Bioresour. Technol. 101, 9049–9057.

Pan, B., Huang, P., Wu, M., Wang, Z., Wang, P., Jiao, X., Xing, B., 2012. Physicochemical and sorption properties of thermally-treated sediments with high organic matter content. Bioresour. Technol. 103, 367–373.

Parshetti, G., Kalme, S., Saratale, G., Govindwar, S., 2006. Biodegradation of Malachite Green by *Kocuria rosea* MTCC 1532. Acta Chim. Slov. 53, 492–498.

Patel, R., Suresh, S., 2008. Kinetic and equilibrium studies on the biosorption of reactive black 5 dye by *Aspergillus foetidus*. Biresour. Technol. 99, 51–58.

Rahman, I.A., Saad, B., Shaidan, S., Sya Rizal, E.S., 2005. Adsorption characteristics of malachite green on activated carbon derived from rice husks produced by chemical–thermal process. Bioresour. Technol. 96, 1578–1583.

Sekhar, C.P., Kalidhasan, S., Rajesh, V., Rajesh, N., 2009. Bio-polymer adsorbent for the removal of malachite green from aqueous solution. Chemosphere 77, 842–847.

Temkin, M.I., Pyzhev, V., 1940. Acta physiochim. URSS 12, 327–356.

Wang, Y., Gong, C., Sun, J., Gao, H., Zheng, S., Xu, S., 2010. Separation of ethanol/water azeotrope using compound starch-based adsorbents. Bioresour. Technol. 101, 6170–6176.

Weber Jr., W.J., Morris, J.C., 1963. Kinetics of adsorption on carbon from solution. J. Sanit. Eng. Div. Am. Soc. Civ. Eng. 89, 31–60.